Design and Characterization of 1.8–3.2 THz Schottky-Based Harmonic Mixers

Berhanu T. Bulcha, Jeffrey L. Hesler, *Senior Member, IEEE*, Vladimir Drakinskiy, Jan Stake, *Senior Member, IEEE*, Alex Valavanis, Paul Dean, Lianhe H. Li, and N. Scott Barker, *Senior Member, IEEE*

***Abstract*—A room-temperature Schottky diode-based WM-86 (WR-0.34) harmonic mixer was developed to build high-resolution spectrometers, and multipixel receivers in the terahertz (THz) region for applications such as radio astronomy, plasma diagnostics, and remote sensing. The mixer consists of a quartz-based local oscillator (LO), intermediate-frequency (IF) circuits, and a GaAs-based beam-lead THz circuit with an integrated diode. Measurements of the harmonic mixer were performed using a 2 THz solid-state source and 2.6906 THz QCL. A conversion loss of 27 dB for the third harmonic mixing and a conversion loss of 30 dB for the fourth harmonic mixing were achieved. This is the first development of a wideband WM-86 (WR-0.34) harmonic mixer with a planar Schottky diode integrated on a beam-lead THz circuit that uses a lower LO harmonic factor for 1.8–3.2 THz RF frequency. Furthermore, this result represents the best Schottky-based mixer in this frequency range.**

***Index Terms*—Conversion loss, coupling efficiency, harmonic mixers, responsivity, Schottky diodes, terahertz (THz) circuits.**

I. Introduction

THE development of Schottky diode-based components has shown tremendous progress [1]. Schottky-based mixers have advantages over other types of detection technologies, such as hot electron bolometer or superconductor–insulator–superconductor tunnel junctions [2], [3]. Schottky diode-based mixers can operate at room temperature or cryogenic with wide intermediate-frequency (IF) bandwidth that allows fast modulation [4], [5]. In addition, Schottky-based mixers use compact and planar technology, which produce rugged components for space-based applications; furthermore, these mixers can be operated in a heterodyne or direct detection mode. Fundamental mixers and subharmonic mixers are currently used at the frequencies below 2.5 THz to down-convert RF signals [6]. However, due to the lack of a compact local oscillator (LO) source with sufficient output power that can be used to pump at the fundamental frequency, it is difficult to develop Schottky-based fundamental mixers above 2 THz. For example, a 2.5 THz fundamental Schottky mixer was demonstrated by Siegel *et al.* for a narrow RF frequency operation. The mixer required approximately 5 mW LO power that was pumped by a CO_2 laser and showed a 17 dB conversation loss at the fundamental mixing [7]. Similarly, subharmonic mixers that use antiparallel Schottky diode technology above 1.5 THz require higher power to pump two diodes. Therefore, at higher frequencies, it is important to develop harmonic mixers that can allow the use of LO harmonics to down-convert the terahertz (THz) RF signal. A previous developed Schottky harmonic mixers such as the 1.5 THz and 2.5 THz balanced mixers demonstrated by Erickson *et al.* presented a conversion loss of 55 and 83 dB at the harmonic factor of $N = 16$ and $N = 25$, respectively [8], [9]. Moreover, room temperature superlattice mixers exhibited a conversion loss of 60 dB or more above 2 THz for $N = 18$, and making it difficult to use for sensitive applications [10].

This paper presents the design and characterization of a wideband 1.8–3.2 THz WM-86 (WR-0.34) mixer that uses lower harmonic factors to present lower conversion loss for different applications such as phase locking THz QCLs by down-converting the THz signal to a lower frequency [11], [12]. Since the mixer is central to the phase locking system, development of mixers with low conversion loss is crucial to achieve phase locking at THz frequencies [13]–[15]. Phase locked THz QCL can be used as a compact LO source to build multipixel receivers, heterodyne interferometers, and tunable heterodyne spectrometers with high spectral resolution in the THz frequencies. Furthermore, the harmonic mixer can also be used in the detector mode to characterize the near- and far-field beam patterns, the divergence angle, beam parameter product, beam quality factor, linewidth, and stability of different THz sources. Detailed characterization of the THz source beam is useful to further improve the device design.

Initially, a VDI WM-102 (WR-0.4) fundamental mixer was modified to build WM-102 (WR-0.4) harmonic mixers by adding two different LO waveguide probe designs to couple LO signals for two different waveguide bands and allow harmonic mixing [13]. The first modified harmonic mixer incorporated a WM-1092 (WR-4.3) LO waveguide and waveguide probe used

Manuscript received February 01, 2016; revised April 09, 2016; accepted May 24, 2016. Date of publication August 04, 2016; date of current version August 31, 2016. The harmonic mixer design, fabrication, and testing were supported by Virginia Diode, Inc., by the University of Virginia, and by the University of Chalmers. The fabrication and the initial characterization of the 2.7 THz QCL used to test the harmonic mixer was supported by the Engineering and Physical Sciences Research Council (EPSRC), U.K., under Grant EP/J002356/1 and Grant EP/J017671/1, and by the Royal Society under the Wolfson Research Merit Award WM110032 and Award WM150029.

B. T. Bulcha and J. L. Hesler are with Virginia Diodes, Inc., Charlottesville, VA 22903 USA (e-mail: bulcha@vadiodes.com; hesler@vadiodes.com).

V. Drakinskiy and J. Stake are with the Department of Microtechnology and Nanoscience, Chalmers University of Technology, Gothenburg 412 58, Sweden (e-mail: vladimir.drakinskiy@chalmers.se; jan.stake@chalmers.se).

A. Valavanis, P. Dean, and L. H. Li are with the School of Electronic and Electrical Engineering, University of Leeds, Leeds LS2 9JT, U.K. (e-mail: a.valavanis@leeds.ac.uk).

N. S. Barker is with the Department of Electrical and Computer Engineering, University of Virginia, Charlottesville, VA 22904 USA (e-mail: nsb6t@virginia.edu).

Color versions of one or more of the figures in this paper are available online at http://ieeexplore.ieee.org.

Digital Object Identifier 10.1109/TTHZ.2016.2576686

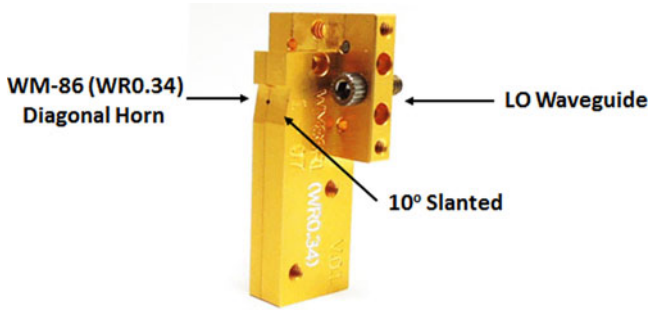

Fig. 1. Harmonic mixer block.

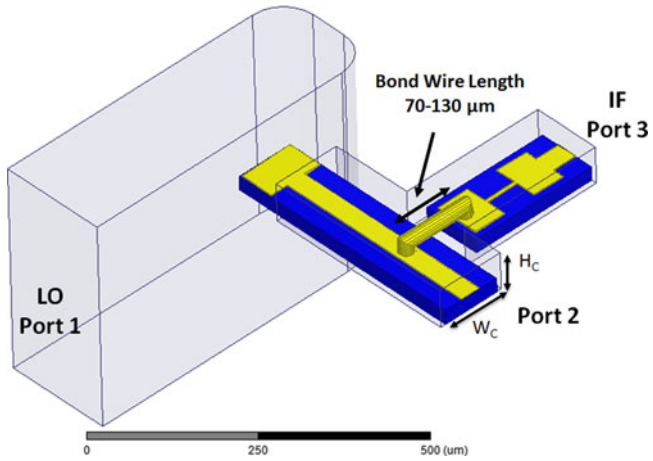

Fig. 2. LO input waveguide with LO probe connected to IF circuit using 1 mil gold bond wire.

to couple 170–260 GHz signals for the ninth and tenth harmonic mixing; a conversion loss of 63 dB was measured. The second harmonic mixer contained a WM-380 (WR-1.5) LO waveguide and waveguide probe designed to couple 500–750 GHz signals for the third and fourth harmonic mixing. This harmonic mixer exhibited poor LO coupling; however, it produced a better conversion loss of 45 dB.

To further improve the performance of the mixer and to broaden the operational frequency, a WM-86 (WR-0.34) harmonic mixer was designed (see Fig. 1). The preliminary design and characterization are presented in [16] and [17]. The next sections detail the design and characterization of the WM-86 (WR-0.34) harmonic mixer that covers 1.8–3.2 THz [see Fig. 3(a)].

II. Harmonic Mixer Design

The initial design of the circuits were modeled and analyzed using advanced design system and High-Frequency Structural Simulator (HFSS) [16], [17]. The harmonic mixer design contained a WM-380 (WR-1.5) LO waveguide. The waveguide had a designed dimension of 190.5 × 381 μm which allowed a 500–750 GHz signal to couple to the LO probe and terminate at the diode. The LO probe used a quartz substrate of 20 μm height and 100 μm width. A 2 μm thick gold conductor was electroplated on top of the quartz substrate to create probe structures. In addition, the LO probe was placed on a waveguide channel with a channel width of $W_c = 125$ μm and a channel height of $H_c = 62.5$ μm. The LO channel dimensions were determined based on the substrate dimensions for a single mode TE_{10} propagation by simulating using an HFSS port solver and determining the starting frequency for all higher modes (see Fig. 2).

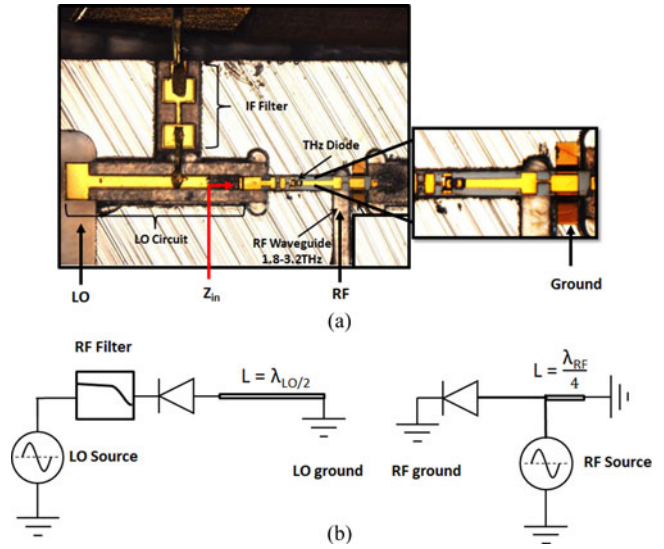

Fig. 3. Harmonic mixer circuitry and equivalent model. (a) 1.8–3.2 THz harmonic mixer internal design. (b) Simple model.

The LO power termination at the diode was provided by a short-circuited beam-lead, located right after the RF-probe, which was clamped between the E-plane split of the block. To maintain the LO termination, the design transmission line length is kept a half-wavelength away from the diode to the short-circuited beam-lead, and the transmission line length is optimized using HFSS [see Fig. 3(a)].

When the mixer was pumped through the LO port, it was important to deliver maximum power by isolating the LO and IF channel; therefore, an IF circuit containing a hi-Z and low-Z based low-pass filters was used to block the LO signal propagation into the IF channel. The IF filter incorporated a 20 μm thick quartz substrate and 2 μm thick gold conductor.

Based on the HFSS simulation result, the transmission, and return loss performance of the IF and LO circuits, at port 1 and port 2, a return loss of 22 dB and an insertion loss of approximately 0.2 dB were obtained. This indicated that more than 95% of the power was coupled into port 1 and propagated to port 2. Similarly, better than 20 dB isolation between port 1 and port 3 was achieved for the 500–750 GHz band.

A. THz Circuit Design

Due to the higher dielectric constant of the GaAs substrate $\epsilon = 12.9$, it was challenging to couple the RF signal as well as to create a lower impedance transmission line that matched with the LO circuit. Therefore, to reduce the effective dielectric constant of the GaAs-based circuit, the THz circuit was floated

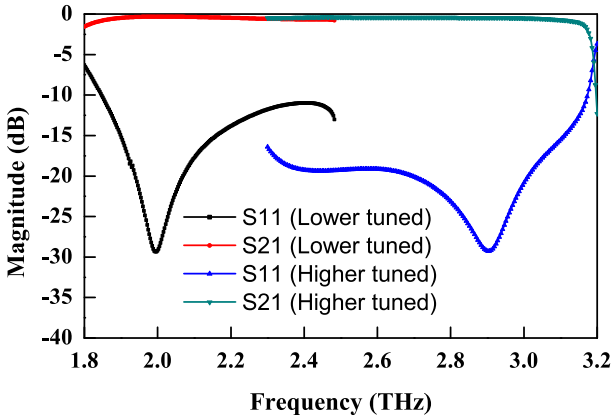

Fig. 4. THz circuit performance (return loss and transmission versus output frequency).

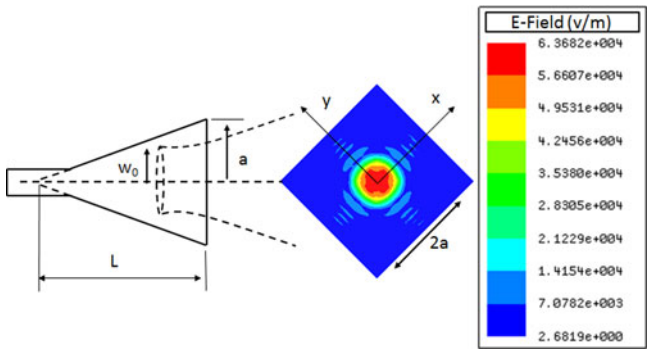

Fig. 5. Schematic of diagonal feedhorn.

above the ground plane to average the dielectric with the air $\epsilon = 1$. Suspending the THz circuit 4 μm above the ground plane reduced the effective dielectric constant to $\epsilon = 2.8$, which was similar to the effective dielectric constant of the quartz-based LO circuits. The THz circuit contained an RF-probe, RF filter, and a single-ended diode [see Fig. 3(b)]. A diagonal-horn antenna with an aperture radius of 0.21 mm fed the RF signal into the RF waveguide, which had a designed dimension of 86.5 $\times$ 43 μm and coupled into the RF-probe. The RF signal propagated through the tapered microstrip transmission line and coupled to the diode.

The RF signal termination was provided by the low-impedance section of the RF filter, which served as a short circuit to the RF signal. To make sure the RF signal propagated only to the RF-probe, an initial quarter-wavelength transmission line (IF/dc path) was added between the probe and the short-circuited beam, and the transmission line length was optimized using HFSS to provide an open circuit to the RF signal at the probe [see Fig. 3(b)] [18].

The RF filter contained five sections of high-impedance and low-impedance transmission lines, with low-impedance dimensions of $W_l = 29$ μm and $L_l = 13$ μm and high-impedance dimensions of $W_h = 2$ μm and $L_h = 13$ μm.

Due to the dc/IF path to ground located between the RF-probe and the short-circuited beam-lead, it was difficult to couple the full RF waveguide band. Therefore, there were two different RF-probe designs to cover from 1.8 up to 3.2 THz. Both probes had similar substrate and probe width. However, due to power coupling at different frequency bands, the two probe structures were different [19]. The lower frequency tuned RF-probe gold structure is within the substrate, whereas the higher frequency tuned RF-probe had a beam-lead with floating gold structure of 5 μm. The simulation performance of the lower band RF-probe design that covered 1.8–2.5 THz and the higher band RF-probe design that covered 2.3–3.2 THz are shown in Fig. 4. The lower band and the higher band RF-probes had a nominal return loss of 15 dB.

During assembly, it was challenging to set the bond wire that connects the IF and LO circuits to the designed length. Therefore, it was important to simulate, by varying the bond wire length, and determine the circuit performance. The LO performance with different bond wire lengths ranging from 70 to 130 μm is simulated and the circuit performance was insensitive to the bond wire length.

It was also critical to analyze the position sensitivity of the THz circuit and its effect on the circuit performance. For the targeted design of a THz circuit floating height of 4 μm, assembly was difficult to achieve. The surface roughness of the THz circuit waveguide channel could introduce 2–3 μm error that might lead to a final 6–7 μm floating height. Therefore, a simulation was set up for floating heights of 2–11 μm and a 0–3 μm left and right lateral position variation of the circuit. The S_{11}performance for both cases was better than -10 dB and the S_{12} was approximately 0.2 dB, which was still within acceptable efficiency range.

B. Diagonal-Horn Antenna

A diagonal-horn antenna was integrated with the mixer block with a horn length of $L = 3$ mm and an aperture diameter of $2a = 0.56$ mm (see Fig. 5). Since the mixer block was an E-plane split, the horn was placed at the block split to ease the machining process.

To reduce the standing wave at the horn surface due to the uncoupled THz beam reflected of off the diagonal horn, the mixer block at the horn aperture was slanted by 10°. This caused the reflected wave at the horn surface to bounce back at an angle. The modified diagonal-horn antenna full three-dimensional structure was simulated and approximately 27 dB gain at 3.2 THz was found.

III. Fabrication of the THz Circuit

Due to the lower dielectric constant ($\epsilon_r = 4$) and higher mechanical strength, a quartz substrate was preferable for making the THz circuit. However, integrating a GaAs-based diode onto a quartz-based THz circuit was challenging. Therefore, the WM-86 (WR-0.34) harmonic mixer used a GaAs substrate with an integrated diode.

The quartz-based circuits, such as the LO probe, the IF circuits, and the supporting substrate, were fabricated at Virginia Diodes, Inc. The THz circuit that contained the THz diode was based on a GaAs, substrate which Jan Stake group fabricated at

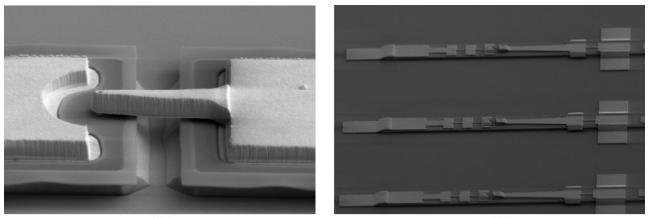

(a) (b)

Fig. 6. 1.8–3.2 THz circuit with beam-lead, fabricated at the Nanofabrication Laboratory, MC2, University of Chalmers. (a) THz diode with 0.4 μm diameter and 6 μm finger length. (b) THz circuit.

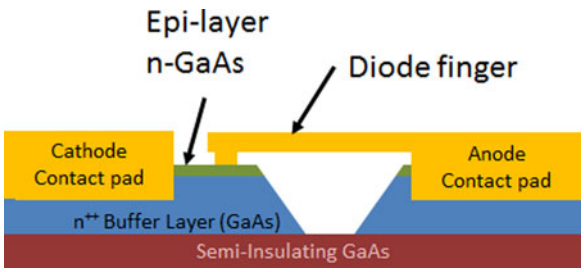

Fig. 7. THz Schottky diode structure.

the Nanofabrication Loaboratory, MC2, University of Chalmers. The diode process was based on electron beam lithography, with a beam spot of less than 5 nm, allowing precise and repeatable anode and air bridge formation.

To achieve a high cutoff frequency and a low conversion loss mixer diode, it was necessary to have high epitaxial doping and small anode size [20]. The THz diode used a 64 nm thick GaAs-based epitaxial layer for its active region with an n-type doping of 3×10^{17} cm^{-3}. At high frequencies, the shunting effect of the junction capacitance over the junction resistor become problematic for the diode performance. As a result, reducing the anode area was necessary to overcome the shunting effect at high frequencies. Therefore, the harmonic mixer contained a THz diode with anode areas of 0.126 and 0.28 μm^2 fabricated for approximately 5–6 μm finger length structures [21], [22]. Scanning electron microscope images of the fabricated THz circuit and the THz diode are shown in Fig. 6.

For diodes on a membrane, the starting structure was a semi-insulating GaAs substrate supporting a 3 μm thick GaAs layer sandwiched in between two AlGaAs etch stop layers and a heavily doped n^{++} buffer layer, followed by an approximately 60 nm n-type epitaxial layer (see Fig. 7). The standard diode fabrication process started with deposition of a stress-balanced PECVD SiO_2 layer, followed by patterning of the ohmic contacts Pd/Ge/Au/Pd/Au. Additional steps, such as annealing of the ohmic contacts and patterning of the Schottky contacts by wet etching through the SiO_2 layer and deposition of Ti/Pt/Au Schottky contacts with following lift-off process were completed. Moreover, patterning the air-bridge and deposition of Au metallization and isolation of the diode by wet etching were performed.

Finally, a formation of the membrane shape and patterning of passive circuitry, such as beam-leads, waveguide probes and

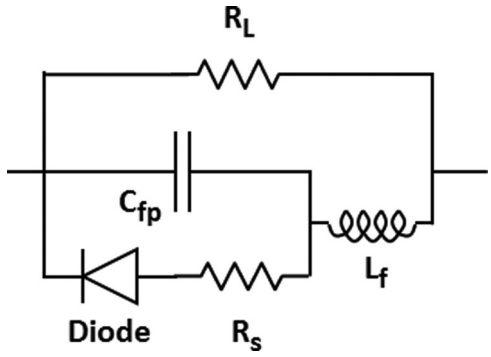

Fig. 8. THz diode model.

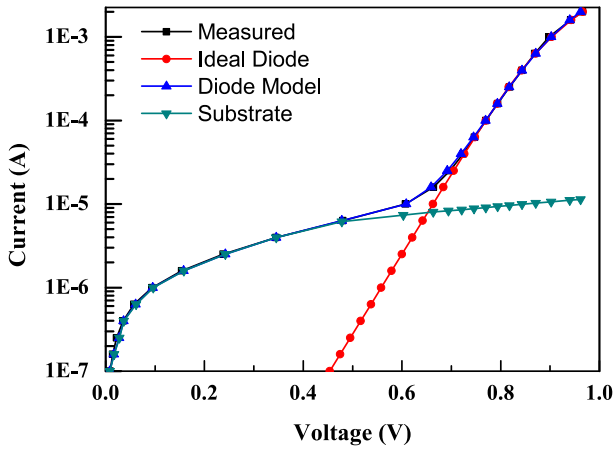

Fig. 9. *I–V* curve of the THz diode compared to an ideal diode to extract important diode parameters.

filter structures, and deposition of thick Au metallization were applied. Thinning down the sample from the backside to the AlGaAs layer which was then etched away to release the devices completed the THz circuit fabrication process [23].

IV. Harmonic Mixer Test and Measured Performance

Test setup and the measured performance of the THz harmonic mixers, such as the current–voltage relationship, RF and LO responsivity, and third and fourth harmonic mixing is presented. Even though the harmonic mixer was designed to work for 1.8–3.2 THz, due to the lack of wide band RF sources, the characterization presented here is for 1.8–2 THz using a solid-state multiplier chain. Harmonic mixer performance above 2 THz was tested using a 2.6906 THz QCL.

Initial harmonic mixer testing was performed by measuring the current–voltage relationships of the THz diode using a Keithley 236 Source-Measure Unit. The current–voltage performance of the THz diode is shown in Fig. 9.

Due to the large substrate leakage resistance, the *I–V* curve was bent for a voltage bias less than 0.6 V. This can be modeled by inserting a shunt resistance across the ideal diode (R_L) and fitting the measured *I–V* characteristics to the model yielding a substrate leakage resistance of approximately $R_L = 80\,\Omega$. For biases greater than 0.65 V, the leakage resistance become

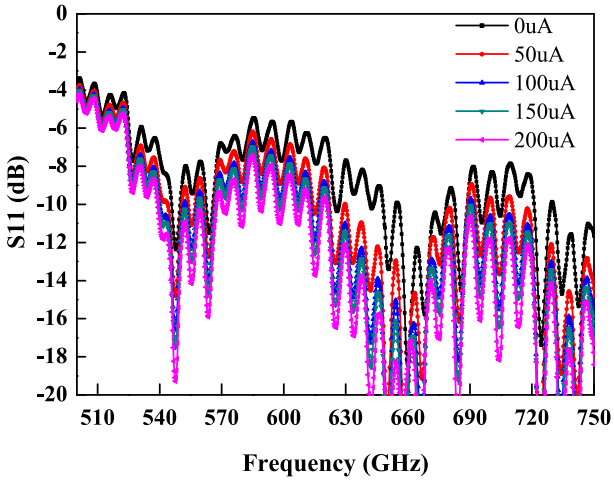

Fig. 10. LO return loss measurement using VNA extender calibrated using SOLT.

insignificant and had no impact on the mixing performance but it affected the small signal detection mode (see Fig. 8).

The diode parameters were extracted by performing a curve fitting to an ideal diode for applied voltage greater than 0.65 V, and minimizing the mean square error for accurate representation. The extracted diode parameters were series resistance $R_s = 27\ \Omega$, ideality factor $\eta = 1.7$, and saturation current under reverse bias $I_0 = 4.2\ pA$.

A. Return Loss and Responsivity

To characterize the LO probe coupling performance and LO power delivery to the diode, LO return loss was measured. Return loss measurements for the harmonic mixer's LO waveguide for different current biases were performed using VDI's WR-1.5 vector network analyzer (VNA) extender, calibrated using VDI's standard SOLT calibration kit. The return loss improved for higher current biases, and showed a nominal return loss better than 10 dB for frequencies above 620 GHz. The performance is illustrated in Fig. 10.

The LO video response was measured by pumping the mixer with LO power while modulating the LO signal and measuring the output voltage on a lock-in amplifier. The LO chain was a VDI solid-state varactor-based amplifier multiplier chain (AMC) source that had an output frequency of 500–750 GHz with a multiplication factor of $N = 48$. The LO source was modulated by a 100 Hz square wave, using a function generator that was connected to a pin-switch within the LO chain. The signal from the function generator was split and used as a reference signal for the lock-in amplifier. The IF chain contained a bias tee that allowed dc bias to the mixer while accessing the modulated video response. The LO video response was tested by pumping the mixer with LO power while biasing the mixer at different current levels. The modulated video output was fed into the lock-in amplifier and the output voltage is measured. From this test, we determined the LO responsivity that relates the input power and the output voltage; the mixer shows better responsivity above 610 GHz (see Fig. 11). Since the available solid-state-based higher frequency multiplier chain

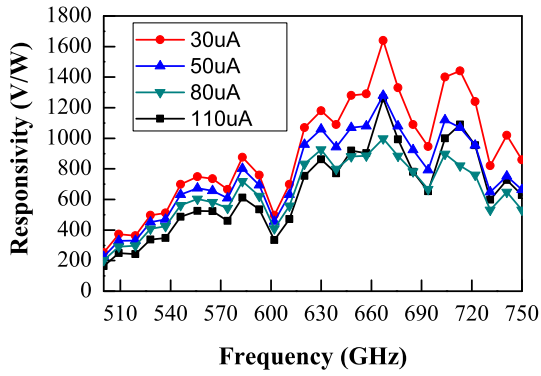

Fig. 11. LO responsivity measurement of the harmonic mixer for different current biases is shown. Due to the calibrated waveguide connections and an active LO input power measurement using a coupler, the measurement uncertainty is neglected.

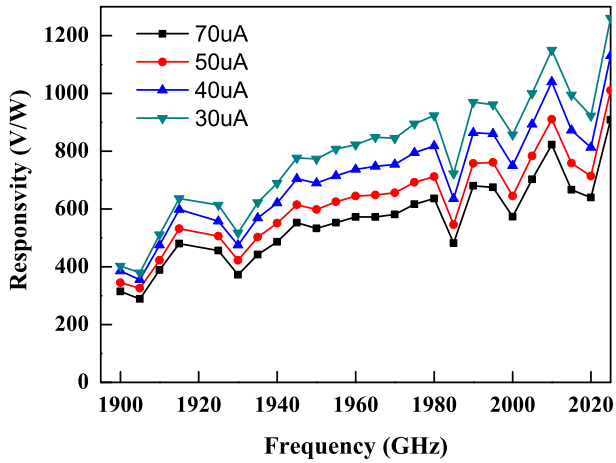

Fig. 12. RF responsivity of the harmonic mixer for different current biases, measurement uncertainty is shown in Table I, adding the uncertainty would change the RF responsivity at 1965 GHz and for a current bias of 50 μA to 600 $\pm$130 V/W.

source matched perfectly to those LO frequencies for the third harmonic mixing, further characterization of the mixer was performed using those LO frequencies.

Similarly, the RF video response for a range of current biases was measured by modulating the RF source using a 100 Hz square wave. We monitoring the modulated video response using the lock-in amplifier. The RF source was a varactor-based multiplier chain with a multiplication factor of $N = 144$. This multiplier chain had an output frequency of 1.9–2.025 THz. The last stage multiplier of the RF source had an integrated WM-130 (WR-0.51) diagonal-horn antenna that transmitted a maximum output power of approximately 2 μW. The power was measured using an Erickson power meter (PM) [24].

The harmonic mixer was set for a range of current biases 30–70 μA. The RF signal was transmitted quasi-optically, and the video response was measured. Finally, responsivity related to the input power and the output voltage was calculated for different current biases.

Fig. 12 depicts the responsivity of the harmonic mixer when it operated in a detector mode by biasing it at lower currents; 30 μA provides the best responsivity. Since 1.9 THz is the

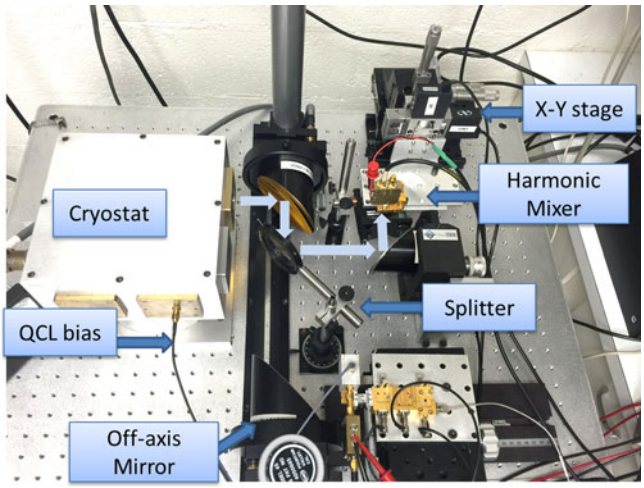

Fig. 13. Video response test setup using 2.6906 THz QCL.

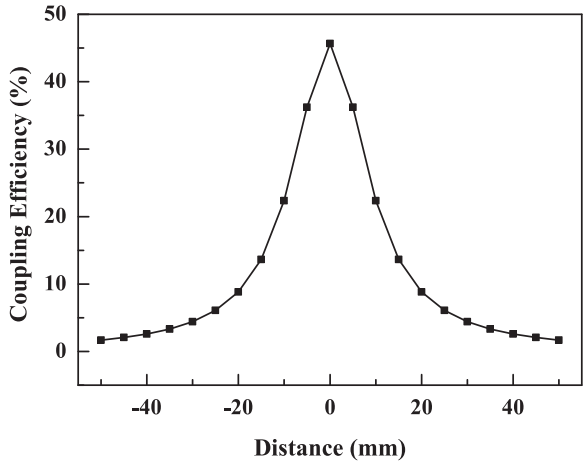

Fig. 14. Coupling efficiency of the harmonic mixer at different position in the optical axis.

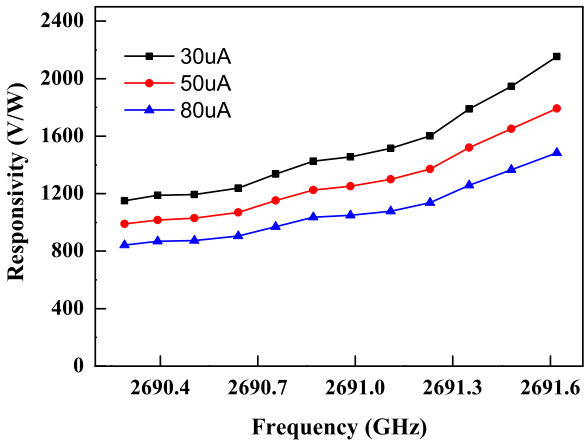

Fig. 15. Responsivity performance of the harmonic mixer tested using approximately 2.6906 THz QCL at different current biases, measurement uncertainty is shown in Table I, adding the uncertainty would change the RF responsivity at 2691 GHz and for a current bias of 50 μA to 1200 $\pm$ 400 V/W.

band edge of the mixer, the responsivity was lower; however, progressing upward in frequency the coupling was better, and the responsivity continuously improved.

The RF video response of the harmonic mixer at 2.69 THz was measured using a QCL as a THz source. The QCL is based on a bound-to-continuum active region, as described in [25], which was processed into a semiinsulating surface plasmon waveguide with 150 micron width and 1 mm length. The QCL was mounted within a Sumitomo SRDK-415D two-stage closed-cycle cryocooler at a heat-sink temperature of 10 K and was driven using a dc current source. The initial mixer test setup was implemented by having two 25.4 $\times$ 76.2 mm 90° off-axis parabolic mirrors collimate and focus the QCL beam (see Fig. 13). The mixer was positioned $\Delta z = 15$ mm away from the focal point of the second mirror to reduce the input power and optimize the video response. An optical chopper was used at the cryocooler window to modulate the THz beam with a 30 Hz modulation rate and then used as a reference for the lock-in amplifier. The QCL was biased at different current values between 0.78 and 0.9 A to generate 2.690–2.6916 THz frequencies with a maximum output power of -7.2 dBm. Since the focused THz beam radius was larger than the mixer diagonal-horn aperture, at $\Delta z = 15$ mm away from the focal point, only up to 10 % of the THz power was coupled to the THz mixer. The coupling efficiency of the harmonic mixer at different position moving closer or further from the QCL facet is depicted in Fig. 14 [26]. The total output power of the QCL was measured using an Erickson calorimeter from VDI, at different frequencies [24]. The coupled power to the harmonic mixer at $\Delta z = 15$ mm was estimated based on the coupling efficiency of the mixer, and it was approximately -17 dBm at 2.69064 THz.

The output video response was recorded from the lock-in amplifier. The input power was estimated from the coupling efficiency of the harmonic mixer, and the responsivity of the mixer was calculated. Fig. 15 depicts the responsivity performance at 2.690–2.6916 THz and different current biases of the harmonic mixer, a nominal responsivity of 1200 V/W was observed. From Fig. 12, 30 μA yielded the best responsivity, which was also the case for the 2 THz responsivity measurements.

This measurement did not account for the uncertainty of the Gaussian coupling efficiency of the receiving horn antenna or the loss due to the transition between the RF waveguide to the microstrip circuit. Similarly, the atmospheric loss in THz frequencies was accounted for in air with 50% relative humidity; however, the humidity might be different during the test, which could change the input power. During the RF power measurement, a VDI Erickson PM with WR-10 straight waveguide and a WR-10 conical horn was used. Since those waveguides were overmoded for the 2.69 THz QCL output power measurement, other modes might have contributed to the power measurement and overestimates the conversion loss data. Due to the difficulty of estimating the power contributions from different modes, it was not accounted for the conversion loss calculation.

B. *Harmonic Mixing at 2 THz*

Due to the lack of a broadband RF source that covers 1.8–3.2 THz, harmonic mixing was tested in two different fre-

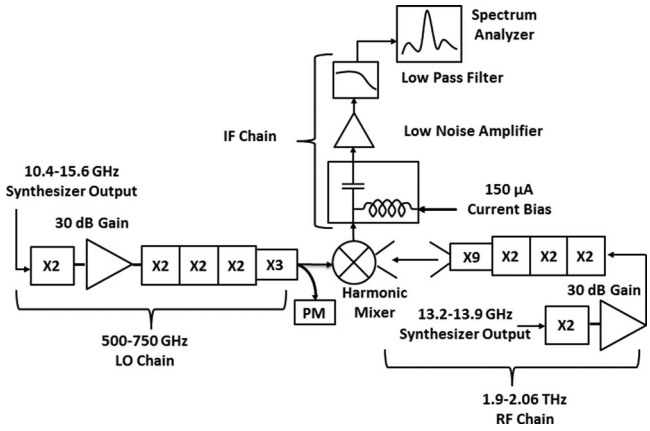

Fig. 16. Experimental setup for harmonic mixing at 2 THz using solid-state sources.

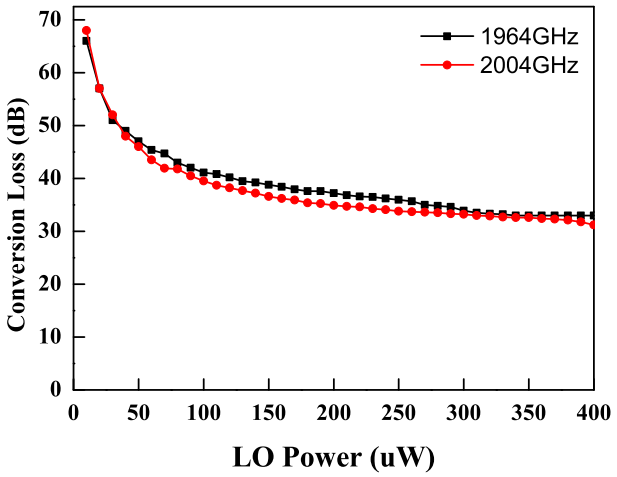

Fig. 17. Above graph shows the third harmonic mixing for two different mixers at LO: 2.0035 THz and RF: 2.004 THz for a fixed current bias of 150 μA.

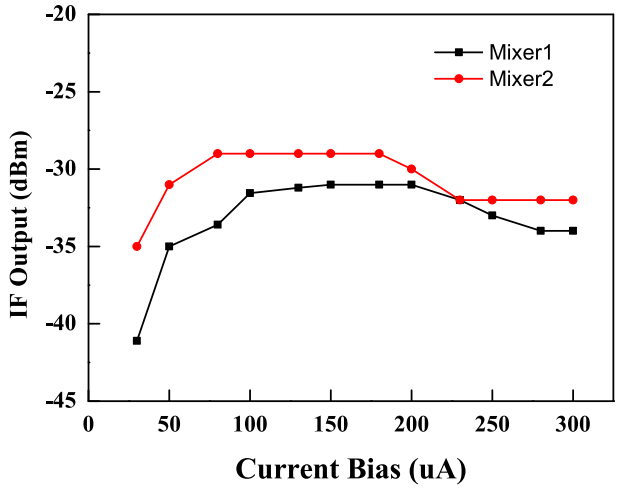

Fig. 18. Mixer's performance (IF output versus current bias) for 380 μW LO power.

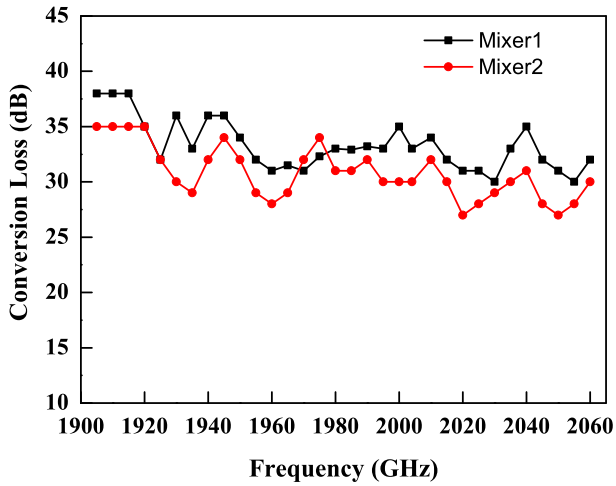

Fig. 19. Optimized conversion loss versus RF frequency.

quency bands. The first harmonic mixing was performed using VDI's 2 THz solid-state source, and the second harmonic mixing was tested using a 2.69 THz QCL (see Fig. 16). Once the RF and LO video response were tested as discussed in the previous sections, selecting the appropriate LO harmonics and RF frequencies based on the video response was straightforward. Harmonic mixing was performed by injecting the RF and LO signal into the mixer and using a spectrum analyzer to monitor the output IF signal. The mixer was biased with different current biases between 150 and 300 μA, and the optimal bias range was determined.

Two different harmonic mixers were characterized and their performances are depicted in Fig. 17. Harmonic mixing was applied using a third harmonic of the 654.5 GHz LO signal that mixed with a 1.9634 THz RF signal. Similarly, a third harmonic of the 667.8 GHz LO signal was mixed with a 2.004 THz RF signal. The down-converted 500 MHz IF signal passed through IF low noise amplifiers with a total gain of 30 dB. To eliminate spurious products and to reduce noise bandwidth, a low-pass filter was used. The IF signal output power was measured using a spectrum analyzer, and the conversion loss was determined.

The performance of the first mixer at different current biases between 30 and 300 μA was investigated while pumping the mixer with an optimal LO power of 380 μW. The current bias range of 140–170 μA was found to provide an optimal IF output power, as shown in Fig. 18. For a fixed IF frequency of 500 MHz, the single sideband conversion loss is also calculated at different RF frequencies. Fig. 19 depicts the optimal conversion loss for different frequencies, ranging from 1.905 to 2.060 THz, by optimizing the LO power and the current bias at each frequency. Conversion loss of 27–35 dB was achieved for the third harmonic mixing, which improved the previous WM-102 (WR-0.4) harmonic mixer conversion loss performance by more than 18 dB.

Measurement uncertainty is shown in Table I; adding the uncertainty for the 300 μW LO drive in Fig. 19 will change the conversion loss by 0.8–2.1 dB.

C. Harmonic Mixing at 2.69 THz

The harmonic mixer performance at higher frequency was tested using a 2.69 THz QCL. The mixer was positioned at

TABLE I.
ESTIMATED MEASUREMENT UNCERTAINTY

Parameter	Uncertainty	Loss (dB)
Gaussian coupling efficiency of the horn (85%)	±3%	0.7±0.1
Loss due to tilt angle	–	0–0.3
Atmospheric loss: relative humidity (50%)	±5%	±1 dB/m
Power measurement accuracy	–	0.2–1

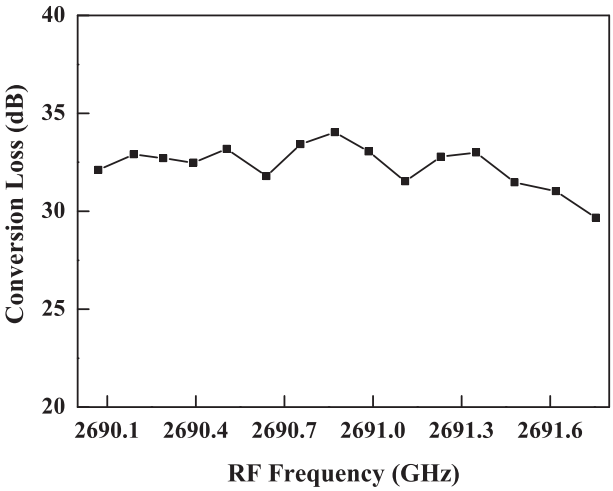

Fig. 20. Conversion loss of the harmonic mixer tested using 2690–2691.8 GHz QCL.

$\Delta z = 15$ mm from the focal point of the second parabolic mirror and the input power estimated from the coupling efficiency of the harmonic mixer and the total output power of the QCL. To measure a constant 1 GHz down-converted IF signal, the fourth harmonic of the LO frequency was varied between 2689 and 2.690.8 GHz and mixed with the QCL frequency of 2690–2691.8 THz. The down-converted 1 GHz IF signal was measured using a spectrum analyzer, and conversion loss was calculated.

Fig. 20 depicts the conversion loss performance of the fourth harmonic mixing and a measured conversion loss of 31–34 dB. Similarly, to measure the IF bandwidth of the harmonic mixer, the LO frequency was swept for a constant RF frequency of 2690 GHz. The LO frequency was varied between 2690.5 and 2730 GHz, and a response of 0.5–40 GHz IF signal was measured. Fig. 21 shows the mixer IF bandwidth performance. The mixer had a fairly flat conversion loss of 30–35 dB up to an IF of 28 GHz, dropped its response between 28 and 36 GHz and returned to a similar conversion loss up to 40 GHz. Measurement uncertainty is shown in Table I; adding the uncertainty will change the conversion loss data shown in Figs. 20 and 21 by 0–3.1 dB across the band.

V. CONCLUSION

A WM-86 (WR-0.34) harmonic mixer was designed for the 1.8–3.2 THz operation. RF performance of the mixer was tested using a 1.9–2.06 THz solid-state AMC source and RF video responsivity of 800 V/W, and a conversion loss of 27 dB for the third harmonic mixing was measured. Similarly, the harmonic

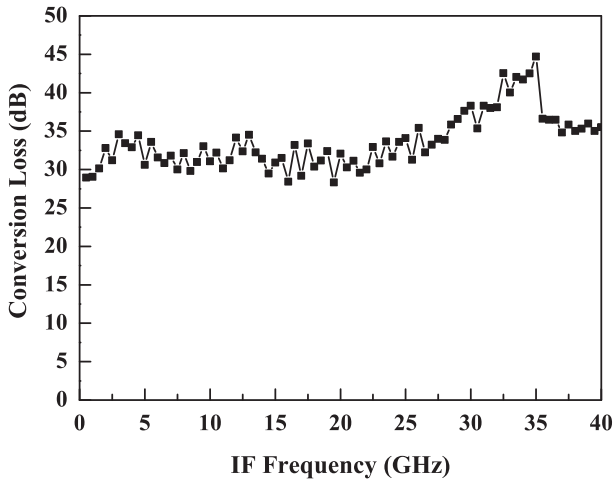

Fig. 21. Conversion loss of a 40 GHz IF bandwidth is tested for a fixed RF: 2690 GHz and LO: 2690.5–2730 GHz.

mixer performance was tested using a 2.6906 THz QCL and a responsivity of 1200 V/W and a conversion loss of 30 dB for fourth harmonic mixing was measured. This result shows a conversion loss improvement of 18 dB from the WM-102 (WR0.4) modified harmonic mixer. Moreover, using this harmonic mixer a 2.5 THz and 2.691 THz QCLs will be phase locked to an external microwave reference.

ACKNOWLEDGMENT

The authors would like to thank R. Dong and J. X. Zhu from the University of Leeds for fabricating and performing initial characterization of the 2.7 THz QCL devices.

REFERENCES

[1] W. Schottky, "Halbleitertheorie der sperrschicht," *Naturwissenschaften*, vol. 26, pp. 843–843, 1938.
[2] S. Bevilacqua, "Superconducting THz mixers based on mgb2 film," Licentiate thesis, THz Millimetre Wave Lab., Dept. Microtechnol. Nanosci., MC2, Chalmers Univ. Technol., Göteborg, Sweden, 2013.
[3] A. Khudchenko *et al.*, "High-gap Nb-AlN-NbN SIS junctions for frequency band 790 to 950 GHz," *IEEE Trans. THz Sci. Technol.*, vol. 6, no. 1, pp. 127–132, Jan. 2016.
[4] H.-J. Song and T. Nagatsuma, Eds., *Handbook of Terahertz Technologies: Devices and Applications*. Singapore: Pan Stanford, 2015, ch. 5.
[5] S. A. Retzloff, A. Young, and J. L. Hesler, "A 1.46 THz Schottky receiver at cryogenic temperatures," in *Proc. 39th Int. Conf. Infrared, Millimeter, THz Waves*, 2014, pp. 1–2.
[6] A. Y. Tang, V. Drakinskiy, P. Sobis, J. Vukusic, and J. Stake, "Modeling of GaAs Schottky diodes for terahertz application," in *Proc. 34th Int. Conf. Infrared, Millimeter, THz Waves*, Sep. 2009, pp. 1–2.
[7] H. P. Riser, "Heterodyne for submillimeter and far infrared wavelength from 100 μm to 500 μm," *Infrared Phys.*, vol. 32, pp. 287–299, Sep. 1986.
[8] N. R. Erickson and T. M. Goyette, "Terahertz Schottky-diode balanced mixers," presented at the 21st Int. Symp. Space THz Technol., Oxford, U.K., Feb. 2009.
[9] A. Danylov, N. R. Erickson, A. Light, and J. Waldman, "Phase locking of 2.324 and 2.959 terahertz quantum cascade lasers using a Schottky diode harmonic mixer," *Opt. Lett.*, vol. 40, no. 21, pp. 5090–5092, Nov. 2015.
[10] D. J. Hayton *et al.*, "Phase locking of a 3.4 THz third-order distributed feedback quantum cascade laser using a room-temperature superlattice harmonic mixer," *Appl. Phys. Lett.*, vol. 103, 2013, Art. no. 051115.
[11] A. A. Danylov *et al.*, "2.32 THz quantum cascade laser frequency locked to the harmonic of a microwave synthesizer source," *Opt. Exp.*, vol. 20, no. 25, 2012, Art. no. 27914.

[12] A. M. Baryshev *et al.*, "Phase-locking of a 2.7-THz quantum cascade laser to a microwave reference," *Opt. Lett.*, vol. 34, pp. 2958–2960, 2009.
[13] B. T. Bulcha, D. S. Kurtz, C. Groppi, J. L. Hesler, and N. S. Barker, "THz schottky diode harmonic mixers for QCL phase-locking," in *Proc. 38th Int. Conf. Infrared, Millimeter, THz Waves*, Sep. 2013, pp. 1–2.
[14] H. W. Hubers, "Terahertz heterodyne receivers," *IEEE J. Sel. Topics Quantum Electron.*, vol. 14, no. 2, pp. 378–391, Mar. 2008.
[15] A. V. Khudchenko *et al.*, "Phase locking a 4.7 THz quantum cascade laser using a super-lattice diode as harmonic mixer," in *39th Int. Conf. Infrared, Millimeter, Terahertz Waves (IRMMW-THz)*, 2014, pp. 1–2.
[16] B. T. Bulcha, J. L. Hesler, and N. S. Barker, "Development of THz harmonic mixer for QCL phase locking application," in *Proc. 39th Int. Conf. Infrared, Millimeter, Terahertz Waves*, 2014, pp. 1–2.
[17] B. T. Bulcha, J. L. Hesler, V. Drakinskiy, J. Stake, and N. S. Barker, " 1.9–3.2 THz Schottky based harmonic mixer design and characterization," in *Proc. Eur. Microw. Conf.*, 2015, pp. 837–840.
[18] C. Risacher, V. Vassilev, A. Pavolotsky, and V. Belitsky, "Waveguide-to-microstrip transition with integrated bias-T," *IEEE Microw. Wireless Compon. Lett.*, vol. 13, no. 7, pp. 262–264, Jul. 2003.
[19] J. L. Hesler, V. Celli, and B. L. Gelmont, "A discussion of power coupling bandwidth limitations of planar Schottky diodes at submillimeter wavelengths," in *Proc. 19th Int. Symp. Space THz Technol.*, 1998, pp. 173–180.
[20] A. Y. Tang, T. Bryllert, and J. Stake, "Geometry optimization of THz sub-harmonic Schottky mixer diodes," in *Proc. 37th Int. Conf. Infrared, Millimeter, THz Waves*, 2012, pp. 1–2.
[21] A. Kerr, "Noise and loss in balanced and subharmonically pumped mixers: Part I—Theory," *IEEE Trans. Microw. Theory Techn.*, vol. 27, no. 12, pp. 938–943, Dec. 1997.
[22] A. Y. Tang and J. Stake, "Impact of eddy currents and crowding effects on high-frequency losses in planar Schottky diodes," *IEEE Trans. Electron Devices*, vol. 58, no. 10, pp. 3260–3269, Oct. 2011.
[23] V. T. Drakinskiy, H. S. Zhao, and P. S. Sob, "Terahertz GaAs Schottky diode mixer and multiplier MIC based on e-beam technology," in *Proc. 25th Int. Conf. Indium Phosphide Related Mater.*, Kobe, Japan, 2013, pp. 1–2.
[24] *VDI PM5 Manual* [Online]. Available: http://vadiodes.com/index.php/en/products/power-meters-erickson
[25] S. Barbieri, J. Alton, H. E. Beere, J. Fowler, and E. H. Linfield, "2.9 THz quantum cascade lasers operating up to 70 K in continuous wave," *Appl. Phys. Lett.*, vol. 85, 2014, Art. no. 1674.
[26] P. F. Goldsmith, *Quasioptical Systems* (IEEE Press Chapman and Hall Publisher Ser. Microw. Technol. and RF). Berlin, Germany: Springer-Verlag, 1998.

Berhanu T. Bulcha received the M.S. degree in electrical engineering from Virginia Commonwealth University, Richmond, VA, USA, in 2011, and the Ph.D. degree in microwave engineering from the University of Virginia, Charlottesville, VA, in 2015.

He is currently a Design and Test Engineer at Virginia Diodes, Inc., Charlottesville, VA, USA. His research interests include development of compact millimeter and submillimeter wavelength devices and systems for different applications.

Jeffrey L. Hesler (S'88–M'89) was born in Seattle, WA, USA, on July 8, 1966. He received the B.S.E.E. degree from the Virginia Polytechnic Institute and State University, Blacksburg, VA, USA, in 1989, and the M.S.E.E. and Ph.D. degrees from the University of Virginia, Charlottesville, VA, in 1991 and 1996, respectively.

He is one of the founding members and a Vice President of Virginia Diodes, Inc., Charlottesville, VA, USA. He is a Visiting Research Assistant Professor with the Department of Electrical and Computer Engineering, University of Virginia. He has authored more than 70 technical papers in refereed international conferences and journals. His research interests include millimeter- and submillimeter-wave device and circuit design, modeling, testing, and development of compact terahertz sources and mixers.

Vladimir Drakinskiy was born in Kurganinsk, Russia, in 1977. He received the Diploma degree in physics and informatics (with honors) from the Armavir State Pedagogical Institute, Armavir, Russia, in 2000, and the Postgraduate degree from Moscow State Pedagogical University, Moscow, Russia, in 2003.

From 2000 to 2003, he was a Junior Research Assistant in the Physics Department, Moscow State Pedagogical University. Since 2003, he has been in the Department of Microtechnology and Nanoscience, Chalmers University of Technology, Gothenburg, Sweden. During 2003–2005, he was responsible for mixer chips fabrication for the Herschel Space Observatory. Since 2008, he has been a Research Engineer with the Department of Microtechnology and Nanoscience, Chalmers University of Technology. He is currently responsible for terahertz Schottky diodes process line at MC2, Chalmers University of Technology. His research interests include microfabrication and nanofabrication techniques, detectors for submillimeter and terahertz ranges, and superconducting thin films.

Jan Stake (S' 95–M' 00–SM' 06) was born in Uddevalla, Sweden, in 1971. He received the M.Sc. degree in electrical engineering and the Ph.D. degree in microwave electronics from the Chalmers University of Technology, Göteborg, Sweden, in 1994 and 1999, respectively.

In 1997, he was a Research Assistant with the University of Virginia, Charlottesville, VA, USA. From 1999 to 2001, he was a Research Fellow with the Millimetre Wave Group, Rutherford Appleton Laboratory, Didcot, U.K. He was then a Senior RF/Microwave Engineer with Saab Combitech Systems AB, until 2003. From 2000 to 2006, he held different academic positions with the Chalmers University of Technology and, from 2003 to 2006, was also the Head of the Nanofabrication Laboratory, Department of Microtechnology and Nanoscience, MC2. During Summer 2007, he was a Visiting Professor with the Submillimeter Wave Advanced Technology Group, Caltech/JPL, Pasadena, CA, USA. He is currently a Professor and the Head of the Terahertz and Millimetre Wave Laboratory, Chalmers University of Technology. He is also a Cofounder of Wasa Millimeter Wave AB, Göteborg, Sweden. His research interests include graphene electronics, high frequency semiconductor devices, THz electronics, submillimeter wave measurement techniques ("THz metrology"), and THz in biology and medicine.

Dr. Stake serves as the Editor-in-Chief of the IEEE TRANSACTIONS ON TERAHERTZ SCIENCE AND TECHNOLOGY.

Alex Valavanis received the M.Eng. (Hons) degree in electronic engineering from the University of York, York, U.K., in 2004, and the Ph.D. degree in electronic and electrical engineering from the University of Leeds, Leeds, U.K., in 2009.

From 2004 to 2005, he was an Instrumentation Engineer with STFC Daresbury Laboratories, Warrington, U.K. He is currently a Research Fellow with the University of Leeds. He is a Member of the Institution of Engineering and Technology. His research interests include quantum cascade lasers, terahertz sensors, silicon photonics, and computational methods for quantum electronics.

Paul Dean received the M.Phys. (Hons.) degree in physics and the Ph.D. degree in laser physics from the University of Manchester, Manchester, U.K, 2001 and 2005, respectively.

In 2005, he became a Postdoctoral Research Associate with the Institute of Microwaves and Photonics, School of Electronic and Electrical Engineering, University of Leeds, Leeds, U.K., and a University Research Fellow, in 2011. His research interests include terahertz optoelectronics, quantum cascade lasers, and terahertz imaging techniques

Lianhe H. Li received the Ph.D. degree in microelectronics and solid-state electronics from the Institute of Semiconductors, Chinese Academy of Sciences, Beijing, China, in 2001.

From 2001 to 2003, he was with the Laboratoire de Photonique et des Nanostructures, Centre National de la Recherche Scientifique, Paris, France, where he was engaged in molecular beam epitaxy growth and characterization of low-bandgap GaAs-based III–V diluted nitride materials and devices with a particular emphasis on 1300–1550 nm telecom wavelength applications. In July 2003, he joined EPFL, Lausanne, Switzerland, as a Scientific Collaborator, where he was involved with InAs quantum dots for lasers and superluminescent LEDs and single quantum dot devices. He is currently with the School of Electronic and Electrical Engineering, University of Leeds, Leeds, U.K.

N. Scott Barker (S'95–M'99–SM'13) received the B.S. degree from the University of Virginia, Charlottesville, VA, USA, in 1994, and the M.S and Ph.D. degrees in electrical engineering from the University of Michigan, Ann Arbor, MI, in 1996 and 1999, respectively.

In 1999, he was a Staff Scientist with the Microwave Technology Branch, Naval Research Laboratory. Since 2001, he has been with the Charles L. Brown Department of Electrical and Computer Engineering, University of Virginia. In 2011, he cofounded the company Dominion MicroProbes, Inc., to develop and market THz frequency technology. His research interests include applying MEMS and micromachining techniques to the development of millimeter-wave and terahertz circuits and components.

Dr. Barker has served on the MTT-21 Technical Committee on RF-MEMS since 2000 and was the Committee Chair from 2008 to 2011. He has also served on the IMS Technical Program Review Committee since 2001. He is currently the Editor-in-Chief for the IEEE MICROWAVE AND WIRELESS COMPONENTS LETTERS.